Coalescence of viscous two-dimensional smectic islands

N. S. Shuravin, P. V. Dolganov, and V. K. Dolganov
Institute of Solid State Physics, Russian Academy of Sciences, Chernogolovka, Moscow Region 142432, Russia

(Received 19 April 2019; published 11 June 2019)

Freestanding smectic films give a unique possibility to study two-dimensional coalescence. We report experimental investigations in freestanding films and detailed analysis of coalescence of islands, circular regions of larger thickness than the surrounding film. The driving force of island coalescence is the dislocation tension on the boundary between the island and the film. The obtained experimental results enable one to perform complex analysis of two-dimensional coalescence in Stokes regime and compare it to theoretical predictions. The applicability of scaling arguments for the description of the peculiarities of domain dynamics is demonstrated. The whole process of coalescence is well described by the analytical solution adapted to our case of islands in freestanding smectic films.

DOI: 10.1103/PhysRevE.99.062702

I. INTRODUCTION

Coalescence of fluid objects is one of the most common phenomena in nature. Different types of coalescence processes can be observed in everyday life; coalescence is widely used in technologies of production of different materials, and it is an integral part of biological processes and natural phenomena. In recent decades coalescence has been extensively studied both experimentally and theoretically. These studies are related to fundamental investigations and have important industrial applications.

Coalescence is a complex phenomenon due to an essential evolution of the structure during the process and the possibility of different dynamical regimes of flow. The first investigations were carried in the 19th century by Rayleigh [1] and Reynolds [2]. The foundations of modern concepts of the evolution of the shape of coalescing domains were laid about 30 years ago in the works of Hopper [3–6]. In the same time numerical calculations of the shape of coalescing particles, dynamics of coalescence were performed [7–9]. Employing numerical methods allows studying the coalescence in complex systems [8], the flow of liquid in microdroplets [10], whose investigation is important for modern technology. Hopper [3–6] obtained a remarkable result, the exact analytical solution for the shape of two viscous cylinders of equal size on different stages of coalescence. This is a unique result since exact solutions in hydrodynamics of complex systems are rarely available. Coalescence was driven by surface tension; the flow was strictly planar. Since the planar-flow dynamics was considered, Hopper's results are also applicable to two-dimensional (2D) coalescence. The obtained solution was exact and rather easy to use, which is why until present time it also remains the basic and useful approximation for analysis of experimental data for three-dimensional (3D) coalescence. By now, numerous experimental and theoretical investigations of coalescence of particles with different viscosity were performed. Experimental investigations of coalescence of 3D droplets confirmed the theoretical predictions of the existence of viscous, so-called "inertial limited viscous" (ILV), and inertial regimes of coalescence [11–14]. The temporal dependence of the radius r_b of a bridge between two droplets at the initial stage of coalescence in these regimes substantially differs. In the ILV regime the dependence of r_b from time is close to linear. If the inertial forces dominate, $r_b \sim t^{1/2}$. Crossover from viscous to inertial regime can be realized with the decrease of material viscosity. Hopper's theory describes coalescence in the viscous regime. It is worth noting however that most experimental investigations were performed on 3D droplets, whereas the majority of theoretical works, including the classical papers of Hopper [3–6], are related to 2D geometry.

Among experimental investigations of 2D coalescence one should note the works of Delabre *et al.* [15] and Delabre and Cazabat [16]. They investigated coalescence of thin nematic domains on a water substrate. The evolution of domains was determined by the dissipation in nematic domains at the initial stage of coalescence; then dissipation in the water substrate dominated. An important step in bringing the experimental conditions close to the 2D situation was made employing freestanding smectic films (FSSF) [17], which are suitable objects for investigations of coalescence [18,19]. In FSSF the two surfaces of the film border with air. Superthin films or nanofilms can be prepared with macroscopic lateral size and thickness from two to tens of molecular layers. To the best of our knowledge, the first experiments of coalescence of smectic islands (regions of larger thickness than the film) were carried out by Nguyen [18]. Analysis of the experimental data and comparison with existing theory was performed [18,19].

The aim of this work is to conduct broader investigations of 2D coalescence and to compare the experimental data with theoretical conceptions at different stages of coalescence. We investigated the coalescence of smectic islands of different size in FSSF over a wide range of times from the contact of

islands to the relaxation of domains toward a circular form. The experimental data allowed directly testing the scaling laws following from theory. We checked experimentally the validity of the two-dimensional viscous analytical solution, obtained by Hopper [3–6], over various ranges of time and size of particles.

II. EXPERIMENTAL DETAILS

In our investigations we used the liquid-crystal 4-n-octylcyanobiphenyl (8CB, Kingston Chemicals). This material has the smectic-*A* (Sm*A*) phase at room temperature. In Sm*A* liquid crystals the molecular long axes are perpendicular to the layer planes. FSSF were prepared by spreading the smectic material across a circular opening in a glass plate. The method employed to obtain the islands in FSSF was described earlier [20,21]. When the islands move in the film due to diffusion and weak air flows in the thermostating stage they can come into contact. After the islands come into contact they, as a rule, remain in this state for some time (in some cases several minutes) before the interface between the islands disappears and coalescence starts. Such behavior is due to the existence of a barrier between the boundaries of islands. Overcoming this barrier by the fluctuational mechanism can take some time. For the investigations of coalescence we selected pairs of coalescing islands with radii $R_{1,2}$ larger than 15 μm, with the same thickness and approximately the same size (with accuracy better than 10%). For two coalescing islands we indicate their average radius $R = (R_1 + R_2)/2$.

Experiments were performed using a Linkam LTS120 heating stage. The island coalescence was recorded with a high-speed Mikrotron EoSens digital camera coupled to an Olympus BX51 microscope. In our investigations the operation mode of the camera was chosen to combine high speed (2500 frames per second) with appropriate spatial resolution and typical frame size 560 × 374 pixels. The microscope was also equipped with an Avantes fiber-optic spectrometer. The number of layers in the film N_f and in the islands N was determined by measurements of the spectra of reflection of nonpolarized light from the film and islands [17].

III. RESULTS AND DISCUSSION

After two islands touch and come into contact [Fig. 1(a)] the gap between the islands can disappear and a bridge between them forms and grows. This is the beginning of coalescence. Figure 1 illustrates the coalescence of two islands with the same thickness and close sizes ($R_1 = 25.2\,\mu$m, $R_2 = 25.5\,\mu$m). During coalescence a complex evolution of the island shape takes place. First we should understand which dynamical regime (viscous or inertial) could be expected during coalescence of islands in FSSF. Inertial forces are negligible compared to viscous forces if the dimensionless group $\rho\gamma R/\eta^2$ is small [3], where ρ is the density, η is the dynamic viscosity. $\rho\gamma R/\eta^2$ is the ratio of the square of Reynolds number to Weber number [3]. In theories describing 3D coalescence of droplets γ is the surface tension for the bulk sample. In our case the boundary between the smectic film and the island is an edge dislocation. The driving force

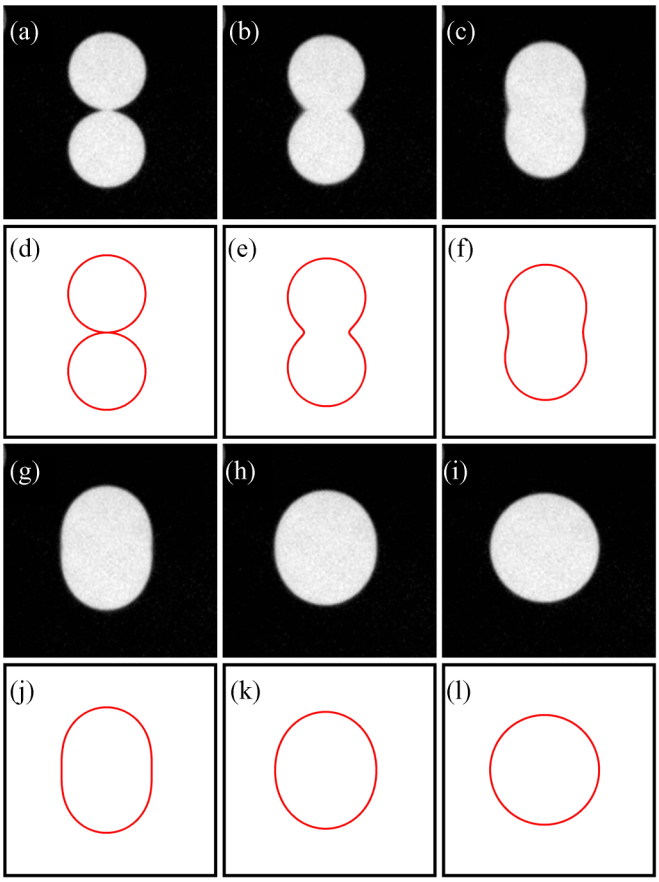

FIG. 1. Coalescence of two smectic islands with the same thickness and close size. (a) Contacting islands before coalescence. Images taken at times after start of coalescence about 0.6 ms (b), 1.4 ms (c), 2.2 ms (g), 3.4 ms (h), and 7.8 ms (*i*). Thickness of the film is 4 smectic layers, thickness of the islands 23 smectic layers, radii of islands before coalescence $R_1 = 25.2\,\mu$m (the upper island) and $R_2 = 25.5\,\mu$m (the lower island). $T = 22\,^\circ$C. (d)–(f), (j)–(l) show the form of the domains calculated using Hopper's model in moments of time corresponding to frames (a)–(c), (g)–(i).

of coalescence is the dislocation line tension. The analog of γ for the dislocation tension is $\gamma_d = \Gamma b/Nd$, where Γ is the line tension of a unit dislocation, that is, dislocation with the magnitude of Burgers vector equal to the smectic layer spacing d, and b is the number of smectic layers in Burgers vector. In our experiments $b/N \sim 0.8$. Taking $\Gamma \approx 10^{-6}$ dyn [22,23] and $d = 3.17$ nm [24] we get for dislocation tension $\gamma_d \approx 3$ dyn/cm. Other material parameters for 8CB are $\rho \approx 1\,\mathrm{g/cm^3}$ [25], $\eta = 0.052$ Pa s [26], and typical radius R is about 40 μm. We get $\rho\gamma_d R/\eta^2 \approx 4.4 \times 10^{-2}$. So, the inertial effects are negligible and coalescence should occur in the Stokes regime.

We start the analysis of experimental data using the theory of Hopper [3–6]. The analytical solution of Hopper is presented by a family of inverse ellipses describing the shape of coalescing particles. The calculation is performed in the assumption that inertial forces are negligible compared with viscous forces. Evolution of the shape at any stage of coalescence was obtained in Cartesian coordinates in parametric

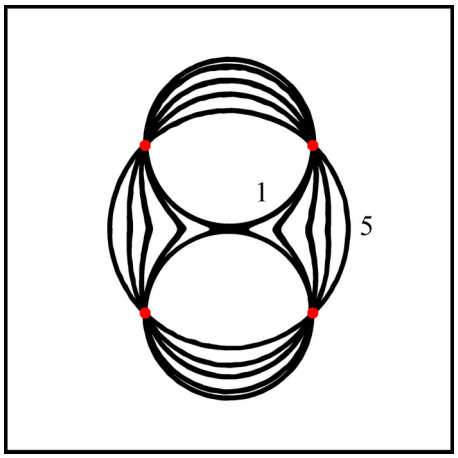

FIG. 2. Evolution of islands during coalescence. Solid curves are the boundaries between the islands and the film. Curve (1) shows two circular islands before coalescence. Curve (5) gives one circular island after coalescence. Images of the domains of other form were taken 0.6, 1.4, and 2.2 ms after the start of coalescence.

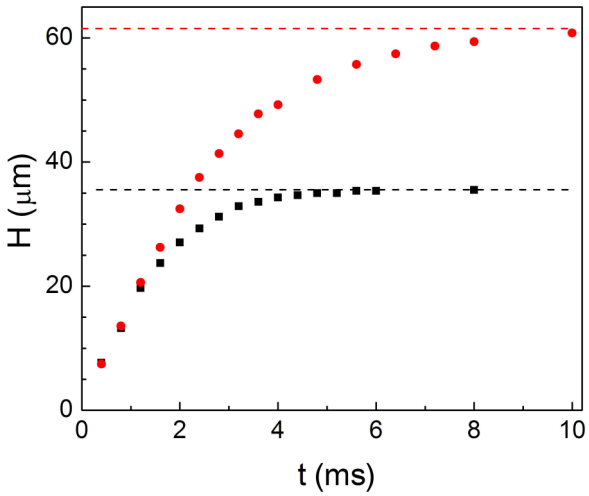

FIG. 3. Time dependence of the half length of the bridge H for two islands with final radius 35.5 μm (■) and 61.5 μm (●). $N = 23$, $b = 19$ (■); $N = 24$, $b = 20$ (●).

representation [3]:

$$x(\theta) = \sqrt{2}R[(1-m^2)(1+m^2)^{-1/2} \times (1+2m\,\cos 2\theta + m^2)^{-1}](1+m)\cos\theta, \quad (1a)$$

$$y(\theta) = \sqrt{2}R[(1-m^2)(1+m^2)^{-1/2} \times (1+2m\,\cos 2\theta + m^2)^{-1}](1-m)\sin\theta, \quad (1b)$$

where m changes from 1 to 0. At $m = 1$ Eqs. (1a) and (1b) describe the initial state of the system (two contacting circles). At $m = 0$ the shape is a circle of final radius $\sqrt{2}R$. For a fixed m the parameter θ varies in the range $0 \leqslant \theta < 2\pi$. Parameter m is related to the time t by an integral equation

$$\gamma t/\eta R = \frac{\pi}{2\sqrt{2}} \int_{m^2}^{1} [\mu(1+\mu)^{1/2}K(\mu)]^{-1} d\mu. \quad (2)$$

Group $\eta R/\gamma$ with dimension t is the characteristic time τ_R. The dependence $K(\mu)$ is determined from the integral equation

$$K(\mu) = \int_0^1 [(1-x^2)(1-\mu x^2)]^{-1/2} dx. \quad (3)$$

Figure 2 illustrates the consequent evolution of islands determined from high-speed camera images. Solid curves are the boundaries between thick domains and the film. According to theory [3] the boundaries are inverse ellipses that intersect at points $(\pm R, \pm R)$. All experimental curves (Fig. 2) as theory predicts intersect at these points.

In many experiments the measured value is the half length of the bridge $H(t)$. Its dependence from m is [3]

$$H(t) = \sqrt{2}R(1-m)(1+m^2)^{-1/2}. \quad (4)$$

First we focus on the time dependence of the bridge size. Its behavior carries information about the mechanism of coalescence, the dependence of the dynamics of the evolution on geometrical parameters of islands. Figure 3 shows the measured dependence of the half length of bridge $H(t)$ for two pairs of islands. Islands in each coalescing pair have close sizes but island sizes in different pairs differ. At short times the flow of material is in general related to the value of the curvature of domain boundary near the two ends of the bridge connecting the islands. At the early stage large curvature leads to high speed of the growth of the bridge length. Then the dynamics slows down and at long times transforms to relaxation towards the equilibrium circular shape. Coalescence time increases with increasing the size of islands (Fig. 3).

The dependence of the bridge half length from time $H(t)$ can be presented by the scaling relation $H(t)/R = F(t/\tau)$. We use the experimental data to check whether coalescence corresponds to the scaling, whether a universal dependence $F(t/\tau)$ from t/τ exists. Points in Fig. 4 are the rescaled

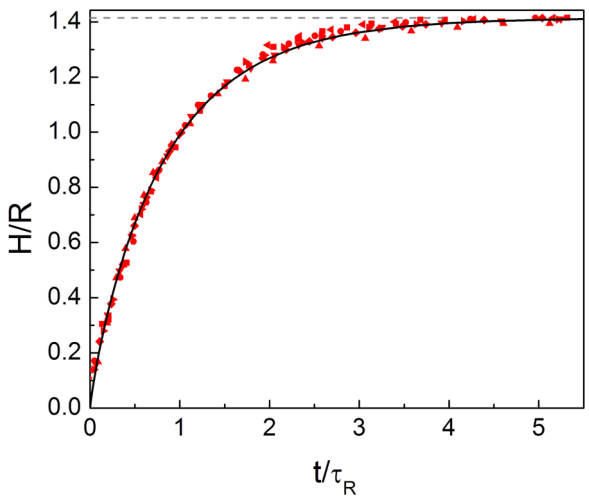

FIG. 4. Time dependence of the half length of the bridge after scaling of H by R and t by τ_R for islands of different size. The solid line is the prediction of Hopper's solution [Eq. (4)]. $R = 25.3\,\mu$m, $N = 23$, $b = 19$ (■), $R = 37.7\,\mu$m, $N = 24$, $b = 21$ (◀), $R = 43.5\,\mu$m, $N = 24$, $b = 20$ (●), $R = 46.0\,\mu$m, $N = 23$, $b = 19$ (♦), $R = 46.4\,\mu$m, $N = 20$, $b = 16$ (▼), $R = 52.1\,\mu$m, $N = 15$, $b = 11$ (▲), $R = 60.2\,\mu$m, $N = 23$, $b = 19$ (▶).

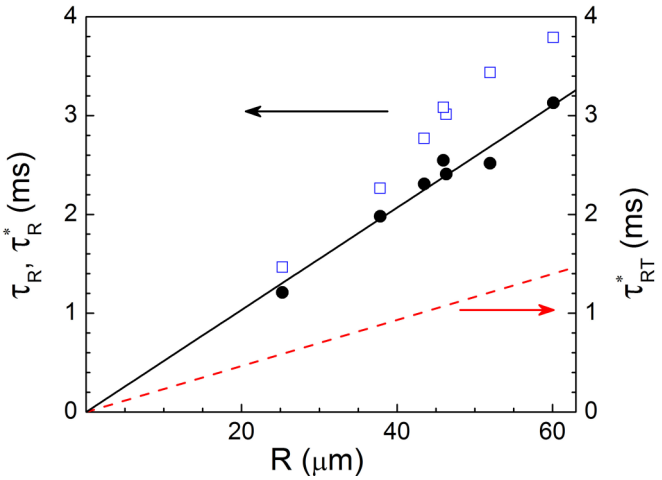

FIG. 5. Dependence of the characteristic time τ_R on island radius R (open squares). Values of τ_R correspond to the data in Fig. 4. Closed circles give the normalized values $\tau_R^* = \tau_R b/N$. The dashed line is $\tau_{RT}^* = \eta R/\gamma_d$ calculated using the material parameters and dislocation tension γ_d.

experimental data $H(t)$ for seven pairs of coalescing islands of different sizes. H was divided by R; the time t was divided by the scaling time τ_R. For every coalescence event the dependence $H(t)/R$ was fitted by Hopper's model [Eqs. (2)–(4)] with fitting parameter τ_R. We found that $H(t)/R$ obtained for different R have the same dependence on t/τ_R (Fig. 4). So, the scaling law is valid for island coalescence dynamics. The solid curve is the dependence obtained from Eqs. (2)–(4). Figure 4 demonstrates that the dependences obtained from coalescence of different islands follows Hopper's dependence. So, we can conclude that (i) the scaling relation $H(t)/R = F(t/\tau)$ is valid, and (ii) the function $F(t/\tau)$ corresponds to Hopper's model.

Open squares in Fig. 5 show the dependence of τ_R from R. In the employed model τ_R is inversely proportional to γ (the energy of the film-island boundary). Note that γ_d and hence τ_R depend on b and N. Closed circles are the normalized values $\tau_R^* = \tau_R b/N$, which, according to theory, should not depend on b and N. Its dependence is found to scale linearly with R, as follows from theory $\tau_R = \eta R/\gamma$ and Hopper's model. However, the absolute values of τ_R^* are considerably larger than $\tau_{RT}^* = \eta R/\gamma_d$ calculated using material parameters and γ_d (the dashed line in Fig. 5). Correction factor is about 2.2. As was pointed in Ref. [19] the deviation in the experimental speed of coalescence from calculated can be connected with dissipation in the film outside the islands and in the surrounding air since the Saffman length l_S [19] is on the order of the island size. Some discrepancy between experiment [18] and Hopper's theory might by due to some uncertainty in the determination of the start of coalescence.

Let us consider in more detail the beginning stage of coalescence. Figure 6 shows rescaled experimental data $H(t)/R = F(t/\tau_R)$ for the early stage of the process (a) and the log-log dependence of $H(t)/R$ from t/τ_R (b). The solid curves are the predictions of Hopper's model. Note that the dependence $H(t)/R$ differs significantly from the 1/2 power

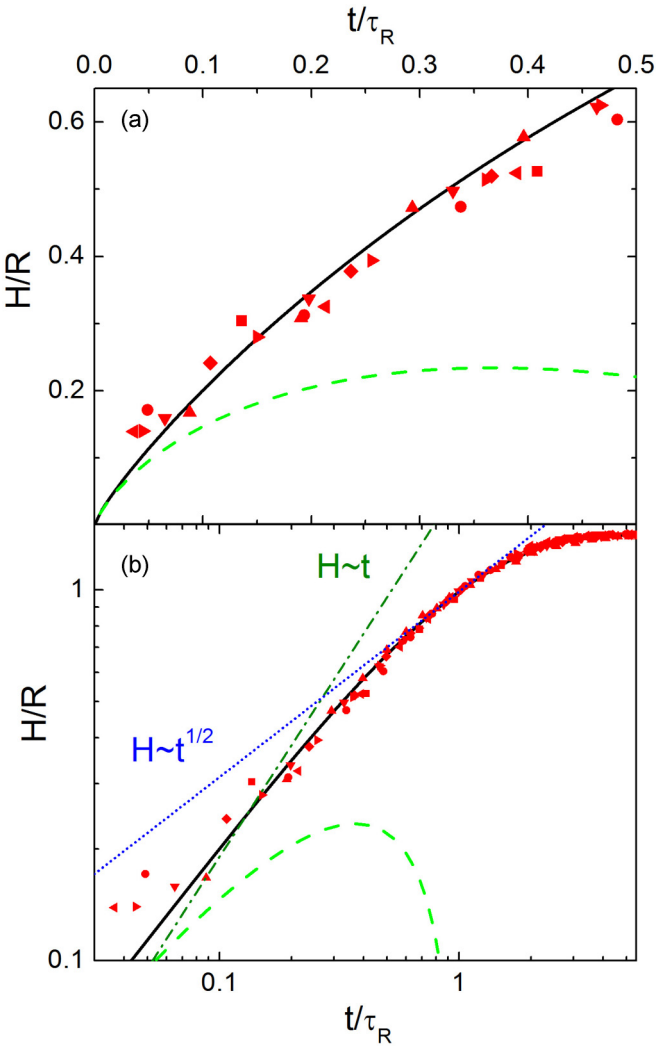

FIG. 6. Initial stage of coalescence for the same islands as in Fig. 4. (a) Dependence of the relative half length of the bridge H/R on dimensionless time t/τ_R for different island sizes. The solid curve is the theoretical prediction by Hopper's model. The dashed curve is the prediction from the scaling law with logarithmical correction $H(t)/R = -t/\pi\tau\ln(t/\tau)$. (b) Log-log dependence of H/R from time. The dash dotted line is $H(t) \sim t$, the dotted line is $H(t) \sim t^{1/2}$, the dashed line $H(t)/R = -t/\pi\tau\ln(t/\tau)$.

law [the dotted line in (b)] which should be expected if inertial forces dominate. So, our evaluation that inertia of the smectic material can be neglected is valid. For the early stage of coalescence in the viscous regime the dependence of H from time was obtained from scaling arguments and numerical calculations [9] and was compared with experiments performed on different types of liquid droplets. From the dependence $H(t)/R = F(t/\tau)$ simple scaling gives a linear variation of H with time $H(t) \sim t/\tau$. Such behavior was found in the investigations of highly viscous 3D liquid droplets [11]. A more exact theoretical description requires a logarithmical correction $H(t)/R = -t/\pi\tau\ln(t/\tau)$ [9,11]. For very short times this equation can be applied for 2D and 3D systems. Such dependence was observed at short times for coalescence of 2D nematic domains on the water substrate [16]. In our

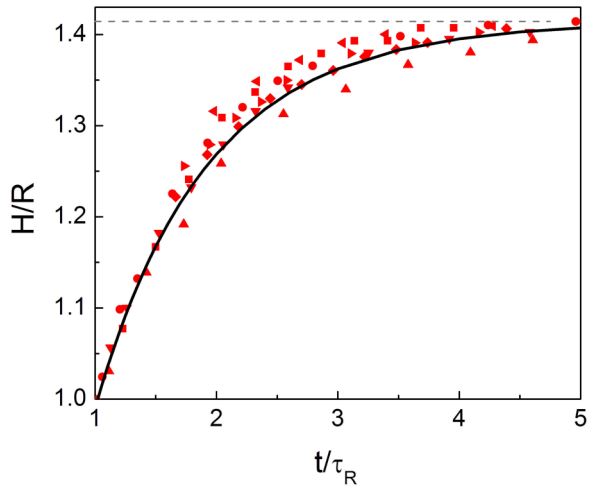

FIG. 7. Final stage of relaxation to the circular shape. Points are rescaled data for the half length of the bridge $H(t)/R$. The solid curve is the prediction derived from Hopper's model.

system this dependence, if it exists, should be expected only at very short times $t < 1$ ms (Fig. 6, dashed curves).

Now attention is paid to the final stage of evolution, that is, relaxation to the circular shape. Points in Fig. 7 show scaled experimental data $H(t)/R$ at the final relaxation stage. We have to stress that scaling times τ_R in Fig. 7 were the same as previously used (in Figs. 4 and 6). According to Hopper's model these dependencies have to be close to exponential. Hopper's solution (the solid curve) well describes the experimental behavior. So, the experimental data in the whole time interval (Figs. 4, 6, and 7) are well described by Hopper's theory. Based on this conclusion we can describe the shape of the domain on different stages of coalescence. Figures 1(d)–1(f) and 1(j)–1(l) show the shape of the domain calculated using Eqs. (1a) and (1b). Calculations were made for the same scaled times t/τ_R as in the above photographs. Good correlation of experimental and calculated shapes is found.

In conclusion, freestanding smectic films opened the way to investigate two-dimensional coalescence. We studied the coalescence of smectic islands in a wide range of time, on different stages of structure evolution. The coalescence dynamics is determined by the competition of the viscosity and line tension related with the dislocation between the island and the film. The obtained results were analyzed using theoretical scaling predictions and the analytical solution for the viscous regime of coalescence. The scaling behavior of the bridge length for islands of different size was established. Times τ_R^* obtained from scaling depend in a linear manner on island radii in accordance with theory. Scaling times τ_R^* are larger than characteristic times calculated from material parameters. For a quantitative description of coalescence, the viscosity of the material in the islands can be replaced by the effective viscosity which is connected with the dissipation in the islands and in the surrounding medium. Hopper's model with Stokes two-dimensional flow can be adapted for a universal description of coalescence process, main characteristics of domains, their shape, and evolution with time. Further investigations are required to understand quantitatively the influence of the outer film and air on the coalescence dynamics.

ACKNOWLEDGMENTS

The reported study was supported by the Russian Science Foundation under Grant No. 18-12-00108. We thank S. V. Filatov for technical assistance.

[1] L. Rayleigh, Proc. R. Soc. London **28**, 406 (1879).
[2] O. Reynolds, Proc. Manchester Lit. Phil. Soc. **21**, 413 (1881).
[3] R. W. Hopper, J. Am. Ceram. Soc. (Commun.) **67**, C-262 (1984).
[4] R. W. Hopper, J. Fluid Mech. **213**, 349 (1990).
[5] R. W. Hopper, J. Fluid Mech. **243**, 171 (1992).
[6] R. W. Hopper, J. Am. Ceram. Soc. **76**, 2947 (1993).
[7] H. K. Kuiken, J. Fluid Mech. **214**, 503 (1990).
[8] G. A. L. van de Vorst, R. M. M. Matteu, and H. K. Kuikens, J. Comput. Phys. **100**, 50 (1992).
[9] J. Eggers, J. R. Lister, and H. A. Stone, J. Fluid Mech. **401**, 293 (1999).
[10] M. Ahmadlouydarab, C. Lan, A. K. Das, and Y. Ma, Phys. Rev. E **94**, 033112 (2016).
[11] D. G. A. L. Aarts, H. N. W. Lekkerkerker, H. Guo, G. H. Wegdam, and D. Bonn, Phys. Rev. Lett. **95**, 164503 (2005).
[12] J. D. Paulsen, J. C. Burton, S. R. Nagel, S. Appathurai, M. T. Harris, and O.A. Basaran, Proc. Natl. Acad. Sci. USA **109**, 6857 (2012).
[13] J. E. Sprittles and Y. D. Shikhmurzaev, Phys. Fluids **24**, 122105 (2012).
[14] J. D. Paulsen, Phys. Rev. E **88**, 063010 (2013).
[15] U. Delabre, C. Richard, J. Meunier, and A-M. Cazabat, EPL **83**, 66004 (2008).
[16] U. Delabre and A-M. Cazabat, Phys. Rev. Lett. **104**, 227801 (2010).
[17] P. Pieranski, L. Beliard, J.-Ph. Tourellec, X. Leoncini, C. Furtlehner, H. Dumoulin, E. Riou, B. Jouvin, J. P. Fénerol, Ph. Palaric, J. Hueving, B. Cartier, and I. Kraus, Physica A **194**, 364 (1993).
[18] D. H. Nguyen, Smectic liquid crystal freely suspended films: Testing beds for the physics in thin membranes, Ph.D. dissertation, University of Colorado, Boulder, 2011, https://scholar.colorado.edu/phys_gradetds/41.
[19] R. Stannarius and K. Harth, in *Liquid Crystals with Nano and Microparticles*, edited by J. P. F. Lagerwal and G. Scalia (World Scientific, Singapore, 2017), pp. 401–405, and references therein.
[20] P. V. Dolganov, N. S. Shuravin, and A. Fukuda, Phys. Rev. E **93**, 032704 (2016).
[21] P. V. Dolganov, E. I. Kats, and V. K. Dolganov, JETP Lett. **106**, 229 (2017).

[22] A. Zywocinski, F. Picano, P. Oswald, and J. Ch. Gèminard, Phys. Rev. E **62**, 8133 (2000).
[23] P. Oswald, F. Picano, and F. Caillier, Phys. Rev. E **68**, 061701 (2003).
[24] D. Davidov, C. R. Safinya, M. Kaplan, S. S. Dana, R. Schaetzing, R. J. Birgeneau, and J. D. Litster, Phys. Rev. B **19**, 1657 (1979).
[25] D. Dunmur and W. Miller, J. Phys. Colloq. **40**, C3-141 (1979).
[26] F. Schneider, Phys. Rev. E **74**, 021709 (2006).